ZANCO Journal of Pure and Applied Sciences
The official scientific journal of Salahaddin University-Erbil
https://zancojournals.su.edu.krd/index.php/JPAS

ISSN (print):2218-0230**, ISSN (online):** 2412-3986**, DOI: http://dx.doi.org/10.21271/zjpas**

RESEARCH PAPER

Effect of thermal axial load on vibration of cracked nanomaterial beam using nonlocal elasticity theory under different boundary conditions

Mohammadtaher M. Saeed Mulapeer *
Mechanical Department, College of Engineering, Salahaddin University-Erbil, Erbil, Iraq

A B S T R A C T:
The aim of this paper is to investigate the free vibration of single-cracked nanomaterials beams under thermal axial load. The beam model is Euler-Bernoulli. The well-known nonlocal elasticity theory is used for analyzing the nanomaterial beams in which the size effect nonlocal parameter is considered. Crack is modeled as a rotational spring that connects the beam segments with each other. The thermal load acts as an axial force on the nanomaterial beam. The effect of the thermal load, the crack location, the crack severity, and the nonlocal parameter are examined in this paper. Two cases of the non-cracked nanomaterial beam and the single-cracked nanomaterial beam are analyzed for three different types of the boundary conditions as simply supported (SS), clamped-clamped (CC), and clamped-simply supported (CS). The results show that when the crack severity is increased the natural frequencies are decreased but in some cases in which the nonlocal parameter value is high, the reverse phenomenon occurs. The temperature changes have a great effect on the frequencies as the temperature is decreased to a value lower than the room temperature, the natural frequencies for all modes decrease and when the temperature is increased to a value higher than the room temperature, the all mode frequencies increase.

KEY WORDS: Free vibration; Single-cracked; Thermal load; Nanomaterial beams; Nonlocal elasticity;
DOI: http://dx.doi.org/10.21271/ZJPAS.33.1.20
ZJPAS (2021) , 33(1);188-204 .

1.INTRODUCTION:

Micro- or nanosized structure properties are very special and this is the reason why they are used in micro- or nanoelectromechanical devices. There are several investigations that are induced different analysis to study the micro- or nanostructures and effect of the different parameters on micro- or nanosized elements such as plates, beams or other membranes. There are several continuum theories in which nanostructures can be analyzed. The nonlocal theory is one the most important continuum theories in which the nonlocal parameter is considered in the equations of this theory. This theory was proposed by Eringen and then it was improved by Eringen and Edelen in the years 1972 and 1983. This theory states that the nonlocal stress-tensor at a point in a body is not only a function of the strain at the same point (local theory), but it is also a function of the strains at all other points of the body (Eringen, 1972, Eringen, 1983, Eringen and Edelen, 1972). The Eringen nonlocal theory was used to derive the equations of the nonlocal Euler- Bernoulli beam for the case of static (Peddieson et al., 2003). Later, the equation of motion was derived to be used for the case of dynamics using the nonlocal theory (Lu et al., 2006). The nonlocal theory could be used for the different types of the beam theories such as Euler-Bernoulli, Timoshenko, and Reddy beam theories. The nonlocal theory could be used to obtain the moment and the shear force equations for Euler-Bernoulli beam (Zhang et al., 2005). Then, the equations of motion for Timoshenko beam using nonlocal elasticity based on the nonlocal bending moment and the local shear force were derived (Wang, 2005, Wang et al., 2006, Wang and Varadan, 2006). The general forms of the equations of motion for Euler-Bernoulli,

* **Corresponding Author:**
Mohammadtaher M. Saeed Mulapeer
E-mail: mohammedtaher.mulapeer@su.edu.krd
Article History: mulapeer@gmail.com
Received: 06/09/2020
Accepted: 11/10/2020
Published: 20/02 /2021

Timoshenko, Reddy, and Levinson beam theories were derived and presented (Reddy, 2007, Reddy and Pang, 2008), and the moment and shear force equations for these beam theories and then, the analytical solutions for bending, buckling, and vibration of the various beam types were presented.

Several researchers applied nonlocal elasticity for dislocation mechanics, wave propagation, and crack problems (Ebrahimi and Barati, 2018, Hussein et al., 2020, Abdullah et al., 2020a, Abdullah et al., 2020b).

Several works have been performed in which vibration of nanostructures such as nanomaterial beams and nanoplates have been investigated using different theories (Eltaher et al., 2013, Hosseini-Hashemi et al., 2015).

The exact solution for large amplitude flexural vibration of nanomaterial beams using nonlocal Euler-Bernoulli theory was presented (Nazemnezhad and Hosseini-Hashemi, 2017).

As well as the single nanorod, investigation of the nonlocal longitudinal vibration of viscoelastic coupled double-nanorod systems (Karličić et al., 2015a) and nonlocal vibration of a piezoelectric polymeric nanoplate carrying nanoparticle via Mindlin plate theory could be also presented (Haghshenas and Arani, 2014).

Several studies have been devoted to the effect of the temperature on the vibration characteristics of the carbon nanotubes and nanomaterial beams. In some of these studies, the nanosized structural element has been embedded in an elastic medium.

In a recent study(Murmu and Pradhan, 2009), the thermo-mechanical vibration of a single-walled carbon nanotube embedded in an elastic medium based on nonlocal elasticity theory was investigated. Investigationg the effects of the thermal load, elastic medium, and magnetic on the vibration of a cracked nanomaterial beam (Karličić et al., 2015b) and functionally graded nanomaterial beams (Ebrahimi and Salari, 2015) showed that the natural frequencies are temperature-dependent and the thermal environment effects cannot be neglected.

A crack acts as a defect in a beam which induces more flexibility to the beam. It is very important to detect the presence, location, size, and number of the cracks in the structural elements to avoid the catastrophic failure. The crack effects on the nanomaterial beams, the nanorods, and the nanoplates have been investigated by many researchers.

Two methods to analyze free vibration of the cracked nanomaterial beams using nonlocal elasticity, as well as using the model of rotational spring for modeling the crack were presented (Loya et al., 2009). The free vibration of multi-cracked nanomaterial beams by a different method was investigated (Roostai and Haghpanahi, 2014) in which the induced flexibility due to the crack, was used instead of the crack severity in calculations.

The free lateral vibration of Euler-Bernoulli nanomaterial beam with multiple discontinuities (Loghmani and Yazdi, 2018) and free transverse vibration analysis of size dependent Timoshenko functional graded (FG) cracked nanomaterial beams resting on elastic medium (Soltanpour et al., 2017) were deeply studied.

Vibration analyzing of multi-cracked nanomaterial beams under thermal environment was recently investigated (Ebrahimi and Mahmoodi, 2018) applying the nonlocal theory. There are some mistakes in mentioned study. As the authors have entered the thermal load in the equation of motion to get the frequencies but after that the thermal load effect has not been induced to the equations of continuity of the bending moment and the continuity of the shear force at the crack location. That is why their results have some errors. According to their results, the frequencies have slightly changed by the large amount of the temperature changes. According to their obtained results, it could be stated that, the frequencies are approximately not temperature dependent and they only depend on the nonlocal parameter and the crack severities.

Furthermore, a noticeable amount of studies has been conducted on the case of the forced vibration analysis.

The forced vibration responses of functionally graded Timoshenko nanomaterial beam using modified couple stress theory with damping effect (Akbaş, 2017) and the forced vibration analysis of a cracked functionally graded microbeam using modified couple stress theory with damping effect were presented (Akbas, 2018).

2. THEORY

2.1 Governing equations for the nonlocal elasticity theory

According to the nonlocal elasticity theory (Eringen, 1972, Eringen and Edelen, 1972), the nonlocal stress-tensor (σ_{ij}) at point x in a body is not only a function of the strain at the same point (local theory), but it is also a function of strains at all other points of the structure. As for the case of homogenous and isotropic nonlocal elastic solid, the general form of equations is written as:

$$\sigma_{ij}(x) = \int \alpha(|\acute{x} - x|, \tau) t_{ij}(x) dV(\acute{x}) \quad (1)$$

The kernel $\alpha|\acute{x} - x|$ is the nonlocal modulus which incorporates into the constitutive relation with the nonlocal effect of the stress at point x created by local strain at the point $\acute{x}$. $|\acute{x} - x|$ is the Euclidean distance. The expressions t_{ij} are the components of the classical local stress tensor at point x. These components have a relation with the local linear strain tensor components ε_{ij} for the materials that obey Hook's law as:

$$t_{ij}(x) = \lambda \varepsilon_{ss}(x) \delta_{ij} + 2G \varepsilon_{ij}(x) \quad (2)$$

The expression τ is the ratio between a characteristic internal length a and characteristic external l length, and $e_o$is a constant which depends on the material and it must be obtained experimentally or by matching dispersion curves of plane waves with those of atomic-lattice dynamics. So, τ is given by:

$$\tau = e_o a / l \quad (3)$$

The integral form of the relation given by Eq. (1) can be represented as a differential form as:

$$[1 - (e_o a)^2 \nabla^2] \sigma_{ij} = [1 - (\tau l)^2 \nabla^2] \, \sigma_{ij} = E\varepsilon(x) = t_{ij}$$
$$\sigma_{xx} - (e_o a)^2 \, \frac{\partial {\sigma_{xx}}^2}{\partial x^2} = E \, \varepsilon_{xx} \quad (4)$$

Where σ_{xx}, is the nonlocal normal stress which differs from the local normal stress t_{xx}; The expressions E and $(e_o a)^2$ are the elastic modulus and the nonlocal parameter respectively. The proposed different model of the nonlocal thermo-elastic constitutive relation (Zhang et al., 2008, Murmu and Pradhan, 2009, Murmu and Pradhan, 2010) in which the nonlocal elasticity theory is combined with the classical thermoelectricity theory is presented in Eq. (5). The constitutive relation for nonlocal viscoelastic solid is given by:

$$\sigma_{xx} - (e_o a)^2 \, \frac{\partial^2 \sigma_{xx}}{\partial x^2} = E \, (\, \varepsilon_{xx} - \frac{\alpha_x \, T}{1 - 2\nu}) \quad (5)$$

Where ν and α_x are the Poisson ratio and the thermal coefficient expansion in x direction respectively and the change in temperature is shown by T. When the amount of $T = 0$, there will not be any effect of the temperature changes in the constitutive relations.

2.2 Nonlocal Euler-Bernoulli beam equations

The displacements for a nanomaterial beam with length L along its axial direction and its vertical directions are:

$$u_1 = u(x,t) - z\,\frac{\partial w}{\partial x}; \qquad u_2 = w(x,t); \qquad u_3 = 0. \tag{6}$$

The expressions u and w are displacements of the nanomaterial beam along the axial and the transverse directions respectively and there is not any motion along third direction (i.e. $u_3 = 0$). Strain in x direction (axial) is given as:

$$\varepsilon_{xx} = \frac{\partial u}{\partial x} - z\,\frac{\partial^2 w}{\partial x^2} \tag{7}$$

Equations of motion for the beam in the axial and the transverse directions, in which the rotary inertia is neglected, are as:

$$\frac{\partial N}{\partial x} + Q(x,t) = \rho A\,\frac{\partial^2 u}{\partial t^2} \tag{8}$$

$$\frac{\partial^2 M}{\partial x^2} + f(x,t) - N\frac{\partial^2 w}{\partial x^2} = \rho A\,\frac{\partial^2 w}{\partial t^2} \tag{9}$$

where N is the applied axial compressive force, $Q(x,t)$ is the horizontal distributed force along the axial direction, M is the resultant bending moment, $f(x,t)$ is the vertical distributed force, ρ is the density, and A is the cross-sectional area of the beam. Where I is the second moment of inertia and V is the shear force. The expressions$N$,M, V, and I are defined as:

$$N = \int_A \sigma_{xx}\,dA; \qquad M = \int_A \sigma_{xx}\,z\,dA; \qquad V = \int_A \sigma_{xy}\,dA; \qquad I = \int_A z^2 dA. \tag{10}$$

The nonlocal form of the axial force, bending moment, and shear force can be written as following (Reddy, 2007, Reddy and Pang, 2008)

$$M - (e_o a)^2\,\frac{\partial^2 M}{\partial x^2} = EI(-\frac{\partial^2 w}{\partial x^2}) \tag{11}$$

The expression $\frac{\partial^2 M}{\partial x^2}$ could be obtained from Eq.(9) as:

$$\frac{\partial^2 M}{\partial x^2} = N\frac{\partial^2 w}{\partial x^2} + \rho A\,\frac{\partial^2 w}{\partial t^2} - f(x,t) \quad \text{(for compressive axial load).} \tag{12}$$

$$\frac{\partial^2 M}{\partial x^2} = -N\frac{\partial^2 w}{\partial x^2} + \rho A\,\frac{\partial^2 w}{\partial t^2} - f(x,t) \quad \text{(for extensional axial force).} \tag{13}$$

Substituting for the second derivative of M from Eq. (13) into Eq. (11), we obtain an equation for the nonlocal moment in which the axial load N is an extensional force.

$$M(x) = -EI\frac{\partial^2 w}{\partial x^2} + (e_o a)^2\left(-N\,\frac{\partial^2 w}{\partial x^2} + \rho A\,\frac{\partial^2 w}{\partial t^2} - f(x,t)\right) \tag{14}$$

Then, the nonlocal shear force can be obtained as:

$$V(x) = -EI\frac{\partial^3 w}{\partial x^3} + (e_o a)^2\left[\frac{\partial}{\partial x}(-N\,\frac{\partial^2 w}{\partial x^2}) + \frac{\partial}{\partial x}\left(\rho A\,\frac{\partial^2 w}{\partial t^2}\right) - \frac{\partial f}{\partial x}\right] \tag{15}$$

Substituting M from Eq. (14) into Eq. (9), we obtain the equation of motion for the nonlocal nanomaterial beam for the lateral displacement in which N is an extensional axial force, as:

$$-EI\frac{\partial^4 w}{\partial x^4} + (e_o a)^2\left[\frac{\partial^2}{\partial x^2}\left(-N\,\frac{\partial^2 w}{\partial x^2}\right) + \frac{\partial^2}{\partial x^2}\left(\rho A\,\frac{\partial^2 w}{\partial t^2}\right) - \frac{\partial^2}{\partial x^2} f(x,t)\right] + f(x,t) + N\,\frac{\partial^2 w}{\partial x^2} = \rho A\,\frac{\partial^2 w}{\partial t^2} \tag{16}$$

For free lateral vibration, all of the lateral external forces must be set to zero, thus, Eq. (16) will be changed and used for lateral vibration as:

$$-EI\frac{\partial^4 w}{\partial x^4} + (e_o a)^2\left[\frac{\partial^2}{\partial x^2}\left(-N\,\frac{\partial^2 w}{\partial x^2}\right) + \frac{\partial^2}{\partial x^2}\left(\rho A\,\frac{\partial^2 w}{\partial t^2}\right)\right] + N\,\frac{\partial^2 w}{\partial x^2} - \rho A\,\frac{\partial^2 w}{\partial t^2} = 0 \tag{17}$$

Assuming the displacement along the axial direction $u = 0$, and the extentional axial load induced by thermal environment N (Karličić et al., 2015b) is as:

$$N = -EA\ \frac{\alpha_x\, T}{1 - 2\nu} \tag{18}$$

One of the following forms of the separation method is used to solve the differential equation of motion as:

$$w(x,t) = W(x)\, T(t) = W(x)\, e^{i\omega t} \tag{19}$$

Let's assume $c^2 = \frac{\rho A}{EI}$ and $r = \frac{EA}{EI}\ \frac{\alpha_x\, T}{1-2\nu}$. The expression ω is the natural frequency of non-cracked nanomaterial beam, then substituting Eq. (19) in Eq. (17) gives:

$$\left[(1 + {e_o}^2 a^2\, r)\ \frac{\partial^4 W(x)}{\partial x^4} - r\frac{\partial^2 W(x)}{\partial x^2}\right] * \frac{1}{c^2\left[W(x) - (e_o a)^2\ \frac{\partial^2 W(x)}{\partial x^2}\right]} = -\frac{1}{T((t)}\ \frac{\partial^2 T(t)}{\partial t^2} = \omega^2 \tag{20}$$

Using following dimensionless variables and constants given by:

$$\varsigma = x/L\ ;\quad h = e_o a/L\ ;\quad \lambda^2 = c^2\omega^2 L^4 = \frac{\rho A\, L^4}{EI}\omega^2;\quad \bar{W} = W/L;\quad q = rL^2 = \frac{EA}{EI}\ \frac{\alpha_x\, T\, L^2}{1-2\nu}. \tag{21}$$

Substituting the dimensionless expressions of Eq. (21) in Eq. (20), we obtain a spatial equation as:

$$\bar{W}^{IV}(\varsigma)(1 + h^2\, q) + (\lambda^2\, h^2 - q)\, \bar{W}''(\varsigma) - \lambda^2 \bar{W}(\varsigma) = 0 \tag{22}$$

We assume $\bar{W} = A\, e^{sx}$ to solve the above differential equation and find its roots as:

$$s^4\ (1 + h^2\, q) + (\lambda^2\, h^2 - q)\, s^2 - \lambda^2 = 0 \tag{23}$$

The roots will be as following:

$$s_1 = i\beta_2;\qquad s_2 = -i\beta_2;\qquad s_3 = \beta_1;\qquad s_4 = -\beta_1. \tag{24}$$

The general solution of Eq. (17) by using Eq. (19) will be as:

$$\bar{W}(\varsigma) = A_1 e^{i\beta_2 x} + A_2 e^{-i\beta_2 x} + A_3 e^{\beta_1 x} + A_4 e^{-\beta_1 x} \tag{25}$$

$$\bar{W}(\varsigma) = C_1 \sinh(\beta_1 \varsigma) + C_2 \cosh(\beta_1 \varsigma) + C_3 \sin(\beta_2 \varsigma) + C_4 \cos(\beta_2 \varsigma) \tag{26}$$

Where β_1 and β_2 are defined as:

$$\beta_1 = \sqrt{\frac{\sqrt{(q+\lambda^2\, h^2)^2 + 4\,\lambda^2} + q - \lambda^2\, h^2}{2(1+h^2\, q)}}\ ;\qquad \beta_2 = \sqrt{\frac{\sqrt{(q+\lambda^2\, h^2)^2 + 4\,\lambda^2} - q + \lambda^2\, h^2}{2(1+h^2\, q)}}. \tag{27}$$

Constants C_1, C_2, C_3, and C_4 in Eq. (26) can be determined through the boundary conditions.
The dimensionless bending slope, dimensionless bending moment and dimensionless shear force can be obtained respectively from Eqs. (26), (14), and (15) using the dimensionless expressions of Eq. (21) as:

$$\theta(\varsigma) = \bar{W}'(\varsigma);$$
$$\bar{M}(\varsigma) = \frac{M(\varsigma)\, L}{EI} = (h^2\, q - 1)\, \bar{W}''(\varsigma) - h^2\, \lambda^2\, \bar{W}(\varsigma); \tag{28}$$

$$\bar{V}(\varsigma) = \frac{V(\varsigma)\, L^2}{EI} = (h^2\, q - 1)\, \bar{W}'''(\varsigma) - (h^2\, \lambda^2 + q)\, \bar{W}'(\varsigma).$$

2.3 Nonlocal cracked Euler-Bernoulli nanomaterial beam equations

It is assumed that a nanomaterial beam has one open edge crack of length t located at a distance $\bar{L}$ from the left end and b= $\bar{L}/L$ (b is dimensionless crack distance from the left end of the beam). A cracked beam is shown in Figure 1 in which a rotational spring is used in the crack location (Loya et al., 2009).

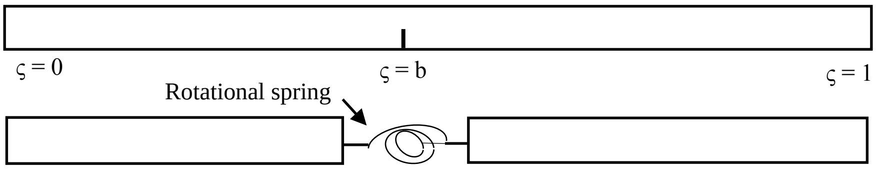

Figure 1. A single-cracked beam model

The crack induces more flexibility to the nanomaterial beam and reduces its stiffness; therefore, a crack can be modeled as a rotational spring. The additional strain energy induced by the crack is as:

$$\Delta \mathcal{U}_c = \frac{1}{2}\, M\, \Delta\theta + \frac{1}{2}\, N\, \Delta u \tag{29}$$

Where $\Delta\theta$ and Δu are the angle of rotation of the rotational spring and the axial displacement of the linear spring respectively. In this paper, the amount of Δu will be zero. Thus, there is only a rotational spring, and parameter $\Delta\theta$ is given by:

$$\Delta\theta = k_{MM}\, \frac{\partial^2 w}{\partial x^2} + k_{MV}\, \frac{\partial u}{\partial x} \tag{30}$$

The crossover flexibility constant k_{MV} is neglected because it is small enough. Now the slope increment $\Delta\theta$ will be rewritten in the form of dimensionless:

$$\Delta\theta = \frac{k_{MM}}{L}\, \frac{\partial^2 \bar{W}(\varsigma)}{\partial \varsigma^2}\bigg|_{\varsigma=b} = K\, \frac{\partial^2 \bar{W}(\varsigma)}{\partial \varsigma^2}\bigg|_{\varsigma=b} = K\, \bar{W}''(b) \tag{31}$$

The expression $K = \frac{k_{MM}}{L}$ is the dimensionless spring stiffness and it is assumed to be the severity of the crack.

Each crack divides the beam into two segments, so if the number of the cracks is increased, the number of the segments will be increased accordingly. Each segment has its own equation of motion as:

$$\bar{W}_1^{IV}(1 + h^2\, q) + (\Lambda^2\, h^2 - q)\bar{W}_1'' - \Lambda^2 \bar{W}_1 = 0 \qquad 0 \le \varsigma \le b \tag{32}$$

$$\bar{W}_2^{IV}(1 + h^2\, q) + (\Lambda^2\, h^2 - q)\bar{W}_2'' - \Lambda^2 \bar{W}_2 = 0 \qquad \mathrm{b} \le \varsigma \le 1 \tag{33}$$

The dimensionless frequency parameter of the cracked nanomaterial beam is shown by Λ , and its relation with the cracked nanomaterial beam natural frequency (ω_c) is as:

$$\Lambda^2 = c^2\, \omega_c^2\, L^4 = \frac{\rho A\, L^4}{EI}\, \omega_c^2 \tag{34}$$

The general solution for the differential Eqs. (32) and (33) for the cracked nanomaterial beam is obtained as:

$$\bar{W}_1(\varsigma) = C_1 \sinh(\beta_s\varsigma) + C_2 \cosh(\beta_s\varsigma) + C_3 \sin(\beta_f\varsigma) + C_4 \cos(\beta_f\varsigma) \quad 0 \le \varsigma \le b$$
$$\bar{W}_2(\varsigma) = C_5 \sinh(\beta_s\varsigma) + C_6 \cosh(\beta_s\varsigma) + C_7 \sin(\beta_f\varsigma) + C_8 \cos(\beta_f\varsigma) \quad \mathrm{b} \le \varsigma \le 1 \qquad (35)$$

Where the coefficients β_s and β_f for the cracked beam are given as

$$\beta_s = \sqrt{\frac{\sqrt{(q+\Lambda^2 h^2)^2+4\Lambda^2}+q-\Lambda^2 h^2}{2(1+h^2 q)}}; \qquad \beta_f = \sqrt{\frac{\sqrt{(q+\Lambda^2 h^2)^2+4\Lambda^2}-q+\Lambda^2 h^2}{2(1+h^2 q)}}. \qquad (36)$$

There are eight unknown constants in Eq. (35), which have to be obtained by exposing the boundary conditions of the beam ends as well as the following compatibility equations at the crack position.

- Continuity of the vertical displacement

$$\bar{W}_1(\mathrm{b}) = \bar{W}_2(\mathrm{b}) \qquad (37)$$

- Jump in Bending slope

$$\Delta\theta = \bar{W}_2'(\mathrm{b}) - \bar{W}_1'(\mathrm{b}) = K\, \bar{W}_1''(\mathrm{b}) \qquad (38)$$

- Continuity of the bending moment

$$(h^2 q - 1)\, \bar{W}_1''(\mathrm{b}) - \Lambda^2 h^2\, \bar{W}_1(\mathrm{b}) = (h^2 q - 1)\, \bar{W}_2''(\mathrm{b}) - \Lambda^2 h^2\, \bar{W}_2(\mathrm{b}) \qquad (39)$$

- Continuity of the shear force

$$(h^2 q - 1)\, \bar{W}_1'''(\mathrm{b}) - (\Lambda^2 h^2 + \mathrm{q})\, \bar{W}_1'(\mathrm{b}) = (h^2 q - 1)\, \bar{W}_2'''(\mathrm{b}) - (\Lambda^2 h^2 + \mathrm{q})\, \bar{W}_2'(\mathrm{b}) \qquad (40)$$

The boundary conditions for the different end supports for a beam exposed to the thermal axial load are as:

- Simply supported end

$$\bar{W}(\varsigma) = 0 \qquad (41)$$
$$\bar{M}(\varsigma) = (h^2 q - 1)\, \bar{W}''(\varsigma) - h^2 \Lambda^2\, \bar{W}(\varsigma) = 0 \qquad (42)$$

- Clamped (fixed) end

$$\bar{W}(\varsigma) = 0 \qquad (43)$$
$$\bar{W}'(\varsigma) = 0 \qquad (44)$$

- Free end

$$\bar{M}(\varsigma) = (h^2 q - 1)\, \bar{W}''(\varsigma) - h^2 \Lambda^2\, \bar{W}(\varsigma) = 0 \qquad (45)$$
$$\bar{V}(\varsigma) = (h^2 q - 1)\, \bar{W}'''(\varsigma) - (h^2 \Lambda^2 + q)\, \bar{W}'(\varsigma) = 0 \qquad (46)$$

It is worth of mentioning that the mode shapes of the nanobeams can be obtained through Eq. (19) in which $w(x,t)$ is the mode shape for the beam deformation, and $W(x)$ is mode function. Once, it is needed to find $W(x)$ which is the dimensional mode function or $W(\varsigma)$ which is the non-dimensional mode function (see Eq. (22)) and then multiply it by the time function $e^{i\omega t}$ to obtain the dimensional mode shape $w(x,t)$ or the non-dimensional mode shape $w(\varsigma,t)$.

1 3. RESULTS AND DISCUSSION

In this paper, the effect of the thermal load as well as the nonlocal parameter, the crack severity, and the crack position is investigated for three different types of the beam supports such as the simply supported, the clamped-clamped, and the clamped-simply supported. The case study of the research of (Roostai and Haghpanahi, 2014) is considered in this paper but in their work the length of the beams was not considered in calculations. In this paper, the length of the nanobeam is $L = 1\, nm$ and the height of the beams is $t = 0.1\, nm$ and the amount of $A/I = 12/t^2$. The amount of the coefficient of thermal expansion is considered as $\alpha_x = -1.6 \times 10^{-6}$ for temperature change equal to or lower than the room temperature and $\alpha_x = 1.1 \times 10^{-6}$ for temperature change higher than the room temperature. As for this work $\alpha_x = -1.6 \times 10^{-6}$ for $T = 0\, K, T = 100\, K$, and $T = 200\, K$, while $\alpha_x = 1.1 \times 10^{-6}$ for the temperature changes higher than the room temperature such as $T = 400\, K$ and $T = 600\, K$ (Yao and Han, 2006). The cases of non-cracked beams are recalculated and the results are tabulated in Table 1 to verify the accuracy of this study and they well agree to the indicated reference (Phadikar and Pradhan, 2010, Roostai and Haghpanahi, 2014).

Table 1. Comparison of the frequencies of non-cracked simply supported nanobeam. ($e_o a = T = 0$).

h	Mode1			Mode2			Mode3		
	Present	(Phadikar and Pradhan, 2010)	(Roostai and Haghpanahi, 2014)	Present	(Phadikar and Pradhan, 2010)	(Roostai and Haghpanahi, 2014)	Present	(Phadikar and Pradhan, 2010)	(Roostai and Haghpanahi, 2014)
0	9.8696	9.8697	9.8700	39.4784	39.4848	39.4780	88.8264	88.8984	88.8260
1	2.9936	2.9936	2.9940	6.2051	6.2061	6.2050	9.3722	9.3796	9.3720

3.1 Simply supported beam (SS)

In this paper, the simply supported (SS) beam is analyzed for the cases of non-cracked and single cracked for the different temperature values. For the case of the single-cracked, the first crack location is $\varsigma = 0.3$ and then, the second position for the crack is chosen to be $\varsigma = 0.5$. The results of the beam with a crack at $\varsigma = 0.5$ are presented Table 2 and they are graphically shown in Figs. 2 and 3. As a crack is introduced to the beam, the natural frequencies decrease and as much as the crack severity increases, the natural frequencies decrease as already reported in several researches (Abdullah et al., 2020a, Hussein et al., 2020). This is because of a reduction in the bending stiffness of the nanomaterial beam due to the presence of the crack. When $T = 0\ K$ (temperature change), it means that the temperature does not have any effects on the frequencies. As much as the temperature increases the frequencies decrease and when the temperature increases to a temperature value higher than the room temperature, the frequencies increase. It is obvious from the results that the temperature can have great effects on the frequencies specially when the amount of the nonlocal parameter increases.

It is observed that when the effects of the crack and the nonlocal parameter are zero (i.e., $K = 0$ and $h = 0$), the temperature change can affect the natural frequencies, but its effect on the first frequency is very significant comparing to the second and third frequencies. As much as the crack severity increases, the frequencies of all modes decrease as shown in Figs. 2, 3, and 4. The reason is that by increasing the crack severity, amount of the additional flexibility introduced by the crack, increases. The highest range of decrease in the frequencies occurs when $h = 1$, $K = 0.075$, and $T = 200$, as it is seen the crack severity and the nonlocal parameter are high values while the value of the temperature change is value lower than the room temperature. The frequencies increase when the crack location is near to the fixed end. Comparing the frequencies of two different crack locations of 0.3 and 0.5, it is observed that when the crack distances from the fixed end, the frequencies of all modes decrease. It means that in the case of the crack location of $\varsigma = 0.3$, the frequencies are higher than the frequecnies of the case in which the crack locates at $\varsigma = 0.5$. It is worth mentioning that the second mode is independent of the crack severity value when the crack locates at $\varsigma = 0.5$. The reason is for the fact that the crack location is exactly the position of one of the nodes of the second mode, consequently, the second mode is independent of the crack severity change in this case because, the amount of the bending slope at both sides of the point on which the crack locates, will be the same, and there will not be any changes and any jumps in the bending slope. The third mode frequencies are not very sensitive to the crack severity when the amount of the nonlocal parameter is higher than zero as shown in Figs 3 and 4, while the first and the second modes are very sensitive to the crack severity at high temperatures and high nonlocal parameter values. Fig. 5 shows a comparison of the first frequency of the different crack locations, in which the amount of K and h are the highest and it is seen that the frequencies are dependent on the crack location. It is interesting to see that at the temperatures equal to or lower than the room temperature, the frequencies of the case of the crack location of

$\varsigma = 0.3$ are higher than the case of the crack location at $\varsigma = 0.5$. At the temperature values higher than the room temperature, the frequency values of the case of the crack location of $\varsigma = 0.5$ are higher than the case of the crack location of $\varsigma = 0.3$.

Table 2. First three dimensionless frequency parameters for a single-cracked simply supported beam with different nonlocal parameter h and different crack severity K. Crack position $\varsigma = 0.5$.

h	T	$K = 0$			$K = 0.0086$			$K = 0.0325$			$K = 0.075$		
		Λ_1	Λ_2	Λ_3	Λ_1	Λ_2	Λ_3	Λ_1	Λ_2	Λ_3	Λ_1	Λ_2	Λ_3
0	0	9.8696	39.4784	88.8264	9.7858	39.4784	88.0824	9.5634	39.4784	86.2059	9.2023	39.4784	83.4368
	100	9.6266	39.2377	88.5861	9.5491	39.2377	87.8483	9.3437	39.2377	85.9880	9.0111	39.2377	83.2448
	200	9.3773	38.9955	88.3451	9.3063	38.9955	87.6134	9.1186	38.9955	85.7694	8.8156	38.9955	83.0523
	400	10.5089	40.1330	89.4840	10.4090	40.1330	88.7233	10.1430	40.1330	86.8023	9.7076	40.1330	83.9622
	600	10.8144	40.4563	89.8110	10.7070	40.4563	89.0420	10.4206	40.4563	87.0989	9.9501	40.4563	84.2234
0.5	0	5.3003	11.9744	18.4390	5.2551	11.9744	18.2819	5.1342	11.9744	17.8632	4.9349	11.9744	17.1943
	100	4.8327	11.1551	17.2441	4.7997	11.1551	17.1279	4.7110	11.1551	16.8167	4.5637	11.1551	16.3101
	200	4.3149	10.2707	15.9600	4.2915	10.2707	15.8755	4.2286	10.2707	15.6482	4.1236	10.2707	15.2732
	400	6.4125	13.9820	21.3833	6.3102	13.9820	21.0269	6.0403	13.9820	20.1066	5.6106	13.9820	18.7881
	600	6.9018	14.8847	22.7128	6.7417	14.8847	22.1529	6.3268	14.8847	20.7660	5.6903	14.8847	19.0097
1	0	2.9936	6.2051	9.3722	2.9681	6.2051	9.2923	2.8996	6.2051	9.0793	2.7861	6.2051	8.7389
	100	2.0553	4.4219	6.7232	2.0487	4.4219	6.7027	2.0307	4.4219	6.6469	1.9996	4.4219	6.5515
	200	0.7771	1.6013	2.3071	0.7771	1.6010	2.3071	0.7771	1.6001	2.3071	0.7771	1.5985	2.3071
	400	4.6893	9.5192	14.3209	4.9808	9.5192	15.2226	5.8963	9.5192	17.0368	7.2657	9.5192	18.0715
	600	5.3389	10.8014	16.2393	5.4728	10.8014	16.6665	5.8712	10.8014	17.8188	6.6411	10.8014	19.2409

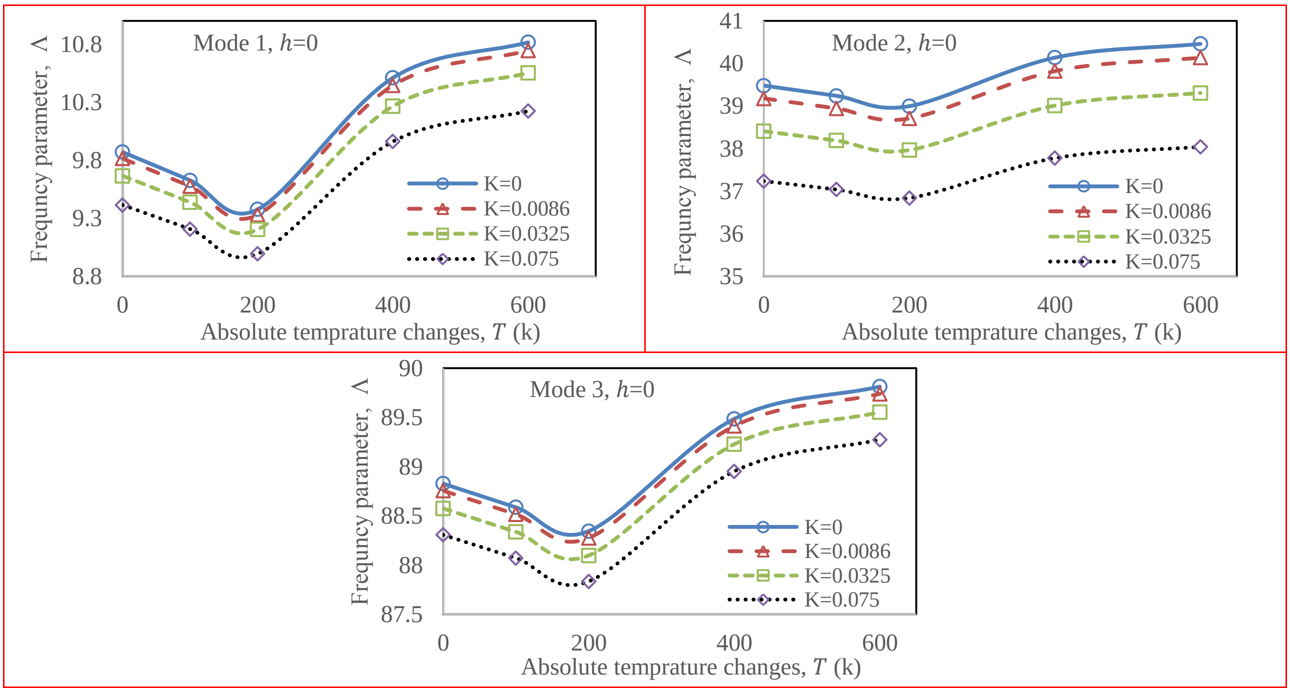

Figure 2. First three frequency parameters for a single-cracked SS beam versus temperature changes. ($\varsigma = 0.3$ and $h = 0$).

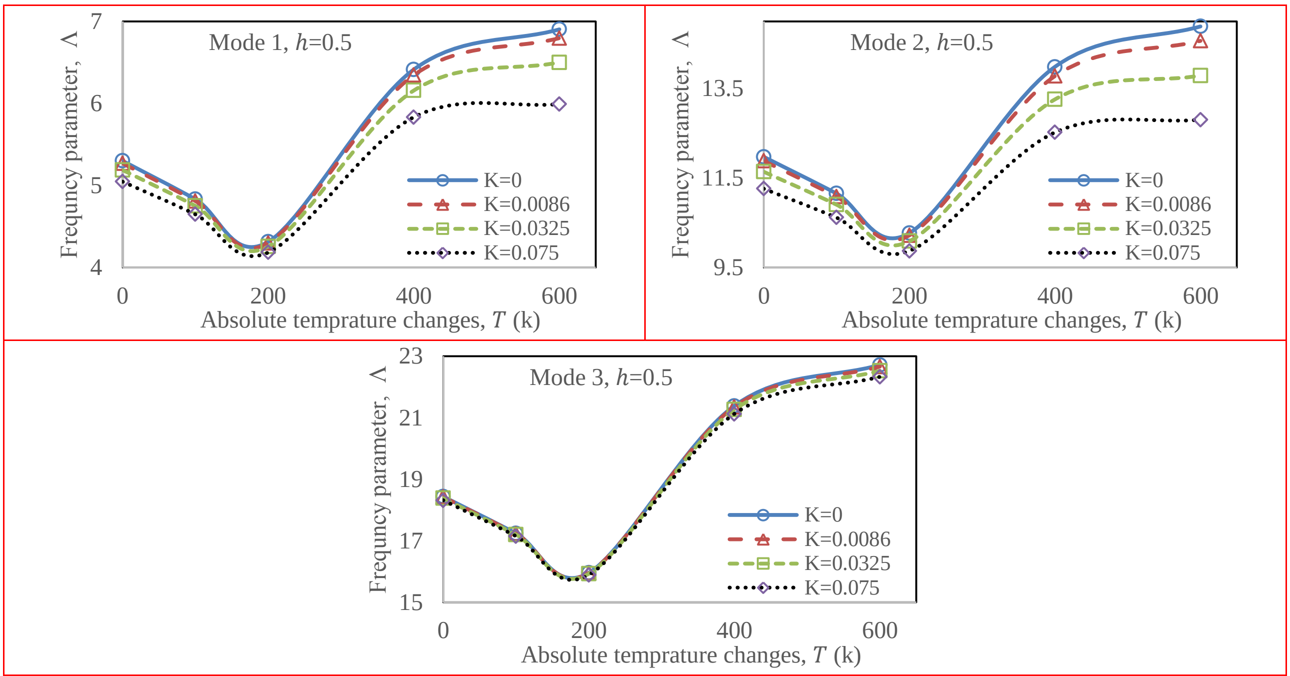

Figure 3. First three frequency parameters for a single-cracked SS beam versus temperature changes. ($\varsigma = 0.3$ and $h = 0.5$).

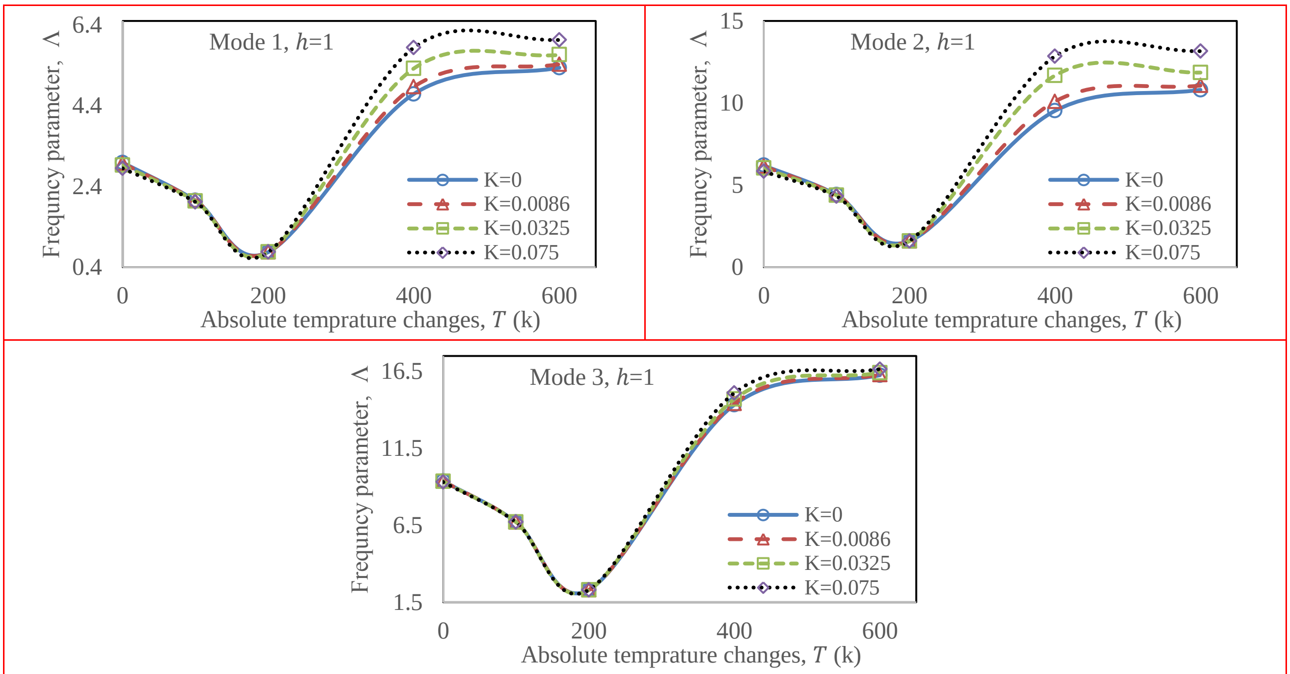

Figure 4. First three frequency parameters for a single-cracked SS beam versus temperature changes. ($\varsigma = 0.3$ and $h = 1$).

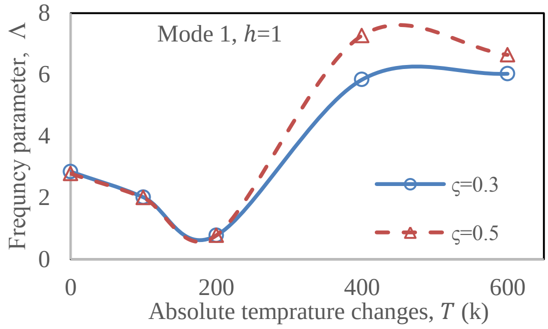

Figure 5. A comparison of the first frequency parameter of a single-cracked SS beam versus temperature changes for two cases of crack positions $\varsigma = 0.3$ and $\varsigma = 0.5$. ($K = 0.075$ and $h = 1$).

3.2 Clamped-clamped beam (CC)

The first three frequency parameters of the clamped-clamped (CC) nanomaterial beams are presented in Table 3 for the crack location of $\varsigma = 0.5$. When the crack location is $\varsigma = 0.3$, all of the frequency modes decrease by increasing the crack severity, and when the nonlocal scale effect parameter (h) increases, the frequencies of all modes decrease. But, when the crack location is $\varsigma = 0.5$, the frequency of the second mode remains constant while the crack severity increases at a certain temperature. The reason is that the point $\varsigma = 0.5$ is a node for the second mode. As the nonlocal parameter increases, the frequencies of all modes decrease. The range of the decrease in the frequencies for the crack location of $\varsigma = 0.5$ is greater than the case of the crack location of $\varsigma = 0.3$ in contrast to non-cracked beam. This is because as the crack location reaches farther from the fixed end, the induced flexibility is increased. However, in some of the cases, especially at higher temperatures, the reverse phenomenon occurs. It is observed that the frequencies are sensitive to the temperature changes. As for the temperatures lower than the room temperature, the frequencies decrease and for the temperatures higher than the room temperature, the frequencies increase. As the crack severity and the nonlocal parameter reach the high values at any temperature, the changes of the frequencies will be significant. The third mode frequency is very sensitive to the temperature changes. The first mode sensitivity to the temperature changes is not as sensitivity as the second and the third modes as shown in Figs. 6 and 7. For a single crack located at $\varsigma = 0.3$, the frequencies of the cases $h = 0.5$ and $h = 1$ approach to each other at the temperatures higher than the room temperature (i.e., $T = 400K$ and $T = 600K$). Thus, it is observed that when the temperature and the crack severity have high values, the effect of the nonzero nonlocal parameter is not significant because the effect of h will be smaller than the effect of the thermal load q in Eqs. (36), (39), and (40). As the amount of the first mode frequency for the higher nonlocal parameter (i.e. $h = 1$) is a higher value in contrast to the lower nonlocal parameter ($h = 0.5$) as shown in Fig. 7. When the temperature is equal to or lower than the room temperature before decreasing to $T = 200K$, the value of the first mode frequency in the case of the crack location of $\varsigma = 0.3$ is higher than the case of the crack location of $\varsigma = 0.5$, but when the temperature reaches a value higher than the room temperature the frequency of the case of the crack location of $\varsigma = 0.5$ is higher than the case of the crack location of $\varsigma = 0.3$ but for the second mode the reverse phenomenon occurs as shown in Fig. 8. Thus, when the temperature change effect is taken into account, it is observed that a higher value of the nonlocal parameter does not always cause in decreasing the frequencies, and the location of the crack is not always a tool to predict whether a certain frequency decreases or it increases.

Table 3. First three dimensionless frequency parameters for a single-cracked clamped-clamped beam with different nonlocal parameter h and different crack severity K. Crack position $\varsigma = 0.5$.

h	T	$K = 0$			$K = 0.0086$			$K = 0.0325$			$K = 0.075$		
		Λ_1	Λ_2	Λ_3	Λ_1	Λ_2	Λ_3	Λ_1	Λ_2	Λ_3	Λ_1	Λ_2	Λ_3

	0	22.3733	61.6728	120.9034	22.2335	61.6728	119.8822	21.8691	61.6728	117.3354	21.2965	61.6728	113.6559
	100	22.2409	61.4933	120.6405	22.1078	61.4933	119.6917	21.7610	61.4933	117.1609	21.2173	61.4933	113.5064
0	200	22.1076	61.3133	120.5445	21.9812	61.3133	119.5009	21.6524	61.3133	116.9860	21.1379	61.3133	113.3566
	400	22.7330	62.1635	121.4406	22.5755	62.1635	120.4044	22.1634	62.1635	117.8140	21.5124	62.1635	114.0656
	600	22.9106	62.4073	121.7239	22.7444	62.4073	120.6646	22.3091	62.4073	118.0525	21.6195	62.4073	114.2697
	0	10.9914	17.2730	24.3324	10.9047	17.2730	24.1141	10.6738	17.2730	23.5350	10.2985	17.2730	22.6344
	100	10.2395	16.1487	22.7861	10.1892	16.1487	22.5961	10.0540	16.1487	22.0911	9.8296	16.1487	21.2915
0.5	200	9.4279	14.9400	21.1269	9.4049	14.9400	20.9613	9.3428	14.9400	20.5204	9.2380	14.9400	19.8130
	400	12.8338	20.0422	28.1501	12.5643	20.0422	27.8130	11.8758	20.0422	26.9344	10.8613	20.0422	25.6996
	600	13.6622	21.2921	29.8766	13.2035	21.2921	29.4290	12.0827	21.2921	28.2942	10.5783	21.2921	26.8740
	0	6.0566	8.8954	12.4530	6.0061	8.8954	12.3451	5.8712	8.8954	12.0590	5.6509	8.8954	11.6158
	100	4.3161	6.3778	8.9537	4.3256	6.3778	8.8813	4.3520	6.3778	8.6870	4.3994	6.3778	8.3656
1	200	2.2934	3.6257	4.9190	0.7744	1.4915	2.2722	0.8185	1.4915	2.2148	0.8981	1.4915	2.1155
	400	9.2913	13.5968	19.0020	10.5666	13.5968	18.9908	10.8138	13.5968	18.9612	11.0453	13.5968	18.9114
	600	10.5428	15.4189	21.5425	11.1657	15.4189	21.4415	13.1919	15.4189	21.1618	15.4189	16.8933	20.5632

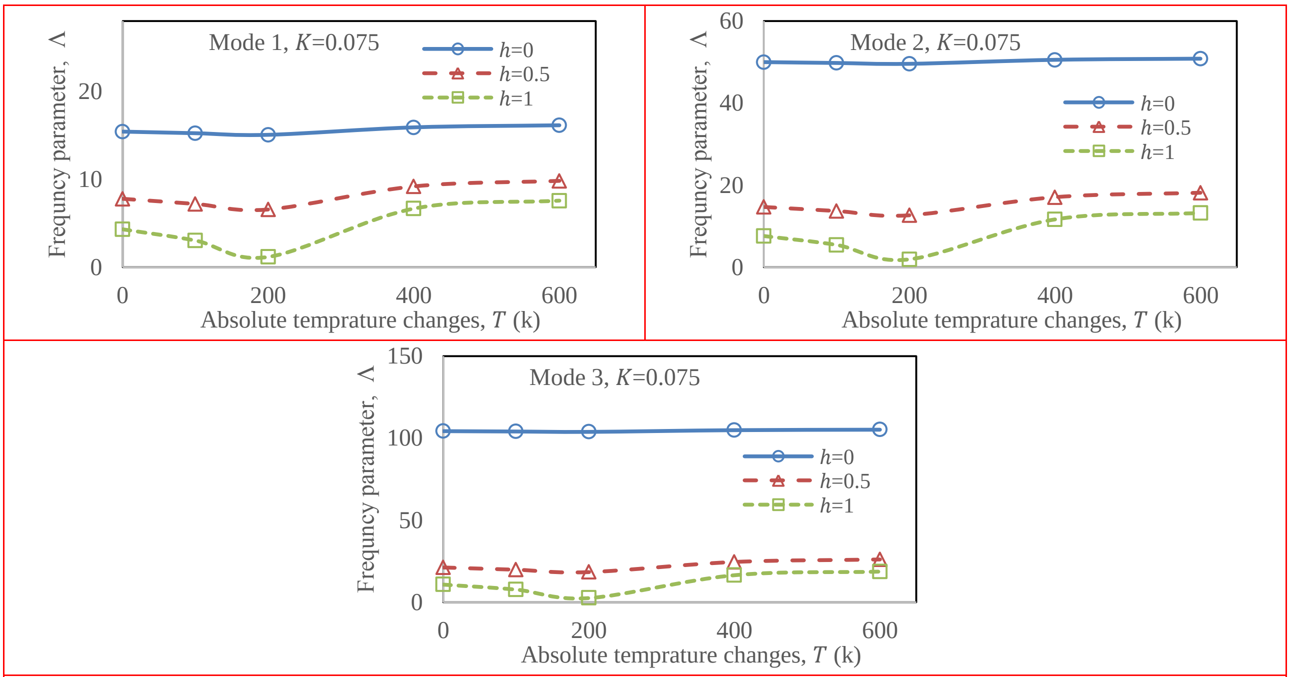

Figure 6. First three frequency parameters for a single-cracked CC beam versus temperature changes for different nonlocal parameters. ($K = 0.075$ and $\varsigma = 0.3$).

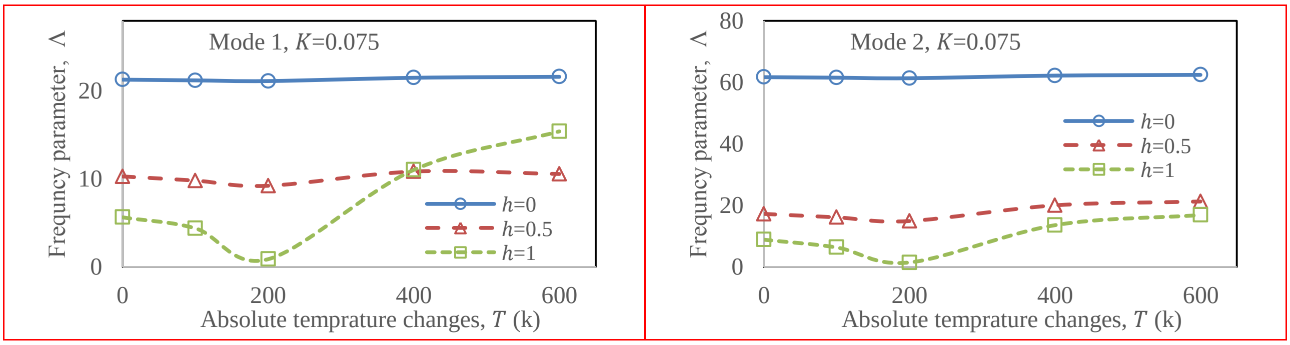

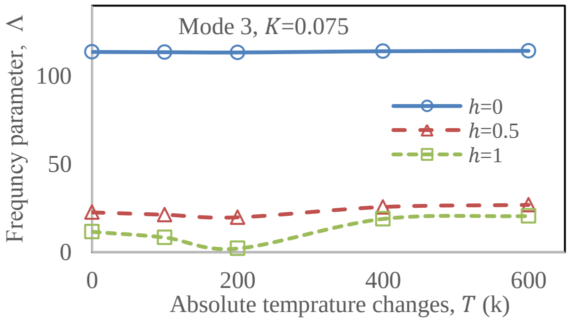

Figure 7. First three frequency parameters for a single-cracked CC beam versus temperature changes for different nonlocal parameters. ($K = 0.075$ and $\varsigma = 0.5$).

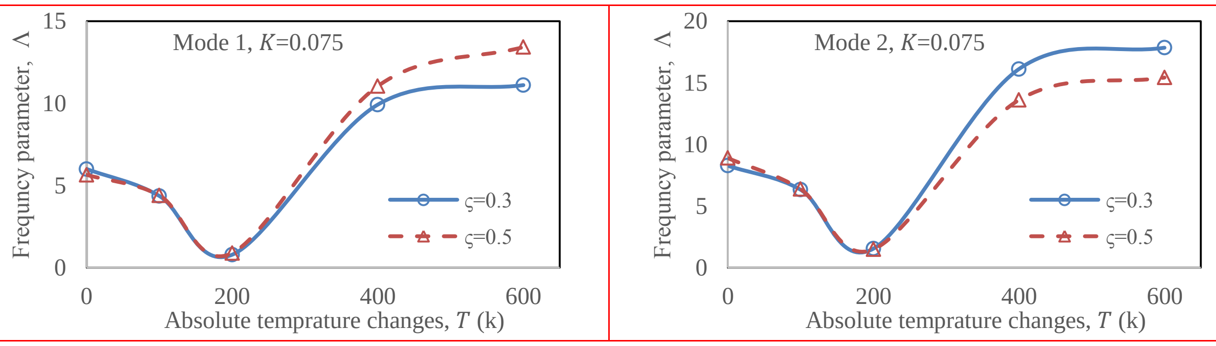

Figure 8. Comparison of first and second frequency parameters of a single-cracked CC beam with temperature changes for two cases of crack positions $\varsigma = 0.3$ and $\varsigma = 0.5$. ($K = 0.075$ and $h = 1$).

3.3 Clamped-simply supported beam (CS)

The results of the clamped-simply supported (CS) beam are presented in Table 4 for the single crack located at $\varsigma = 0.5$. The non-cracked beam results are obtained when the amount of crack severity K is equal to zero. The frequencies of all modes decrease by decreasing the temperature to the values lower than the room temperature and they increase when the temperature increases to the temperature values higher than the room temperature. But when the amount of the nonlocal parameter increases, the changes in the frequencies become more significant as shown in Fig. 9. Modes one and three of the case of the crack location at $\varsigma = 0.3$ are higher than the case in which the crack locates at $\varsigma = 0.5$, but the second mode of the case of the crack location of $\varsigma = 0.5$ is higher than the case of the crack location of $\varsigma = 0.3$. The frequencies of all modes decrease at the temperatures lower than the room temperature and they increase with increasing at the high temperatures. Increasing the nonlocal parameter h results in decreasing the frequencies of all modes as shown in Fig. 10. As the crack severity increases, the frequencies decrease because the flexibility of the beam increases due to the crack; but when the nonlocal parameter h reaches to a very high value (i.e., $h = 1$), the frequencies increase with increasing the crack severity at the temperatures lower and higher than the room temperature but not at the room temperature.

Table 4. First three dimensionless frequency parameters for a single-cracked clamped-simply supported beam with different nonlocal parameter h and different crack severity K. Crack position $\varsigma = 0.5$.

h	T	$K = 0$			$K = 0.0086$			$K = 0.0325$			$K = 0.075$		
		Λ_1	Λ_2	Λ_3	Λ_1	Λ_2	Λ_3	Λ_1	Λ_2	Λ_3	Λ_1	Λ_2	Λ_3
0		15.4182	49.9649	104.2477	15.3288	49.9094	103.4959	15.0935	49.7639	101.6045	14.7167	49.5332	98.8313
	100	15.2379	49.7584	104.0310	15.1544	49.7036	103.2847	14.9350	49.5599	101.4079	14.5847	49.3321	98.6577

0	200	15.0552	49.5510	103.8138	14.9778	49.4969	103.0731	14.7746	49.3550	101.2109	14.4510	49.1304	98.4837
	400	15.9028	50.5283	104.8414	15.7977	50.4711	104.0744	15.5199	50.3209	102.1430	15.0723	50.0821	99.3065
	600	16.1393	50.8076	105.1369	16.0266	50.7496	104.3625	15.7283	50.5972	102.4111	15.2461	50.3544	99.5430
	0	7.7837	14.6881	21.2563	7.7398	14.6431	21.1435	7.6214	14.5202	20.8386	7.4238	14.3127	20.3449
	100	7.2026	13.7153	19.8943	7.1748	13.6872	19.8012	7.0994	13.6100	19.5474	6.9733	13.4766	19.1255
0.5	200	6.5704	12.6680	18.4319	6.5548	12.6527	18.3548	6.5126	12.6103	18.1435	6.4418	12.5358	17.7850
	400	9.1941	17.0799	24.6163	9.0709	16.9496	24.4146	8.7407	16.6086	23.8916	8.2067	16.0971	23.1545
	600	9.8237	18.1580	26.1348	9.6180	17.9394	25.8466	9.0731	17.3941	25.1360	8.2293	16.6748	24.2699
	0	4.3182	7.6211	10.8300	4.2944	7.5940	10.7770	4.2294	7.5202	10.6338	4.1198	7.3964	10.4028
	100	3.0419	5.4530	7.7792	3.0424	5.4550	7.7508	3.0438	5.4609	7.6707	3.0461	5.4718	7.5260
1	200	1.1785	1.9350	2.6263	1.1835	1.9277	2.6185	1.1983	1.9065	2.5987	1.2275	1.8657	2.5687
	400	6.6694	11.6634	16.5351	7.0993	12.2607	16.7464	8.0572	13.8723	17.4086	8.7643	14.8493	18.1202
	600	7.5761	13.2292	18.7476	7.7945	13.5192	18.8106	8.3741	14.4573	19.0170	9.1640	15.9868	19.4641

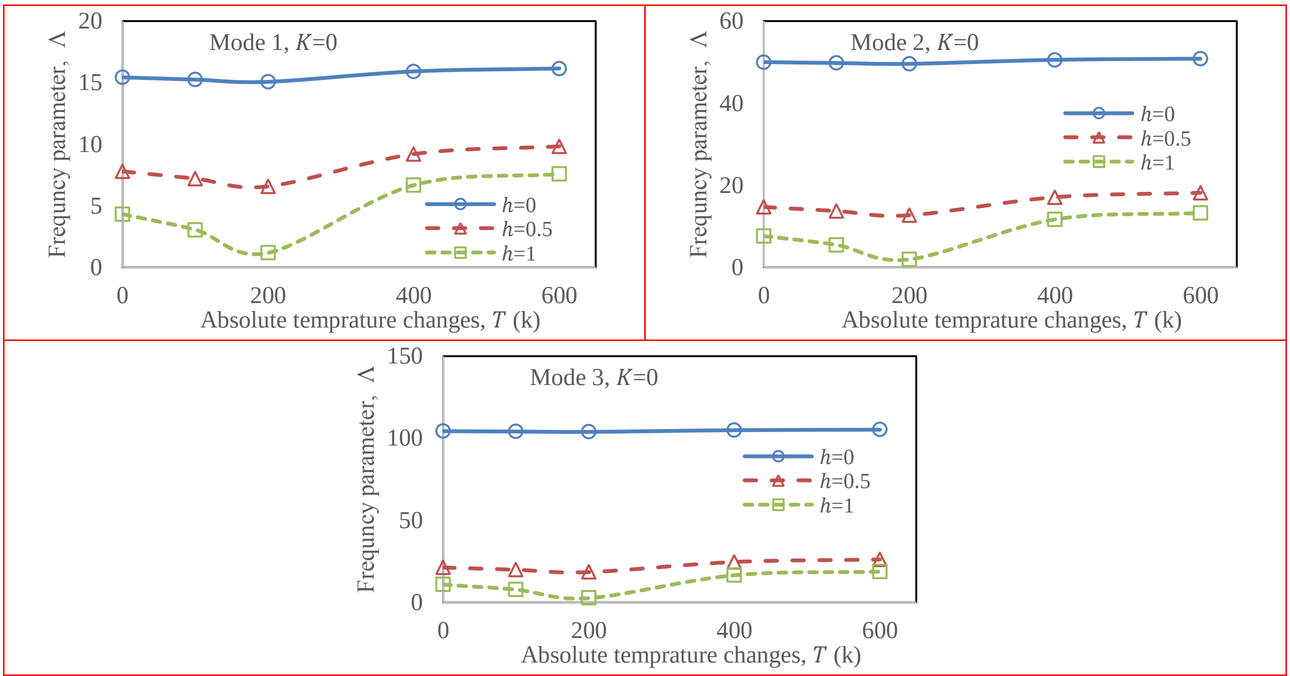

Figure 9. First three frequency parameters for a non-cracked CS beam versus temperature changes for different nonlocal parameters.

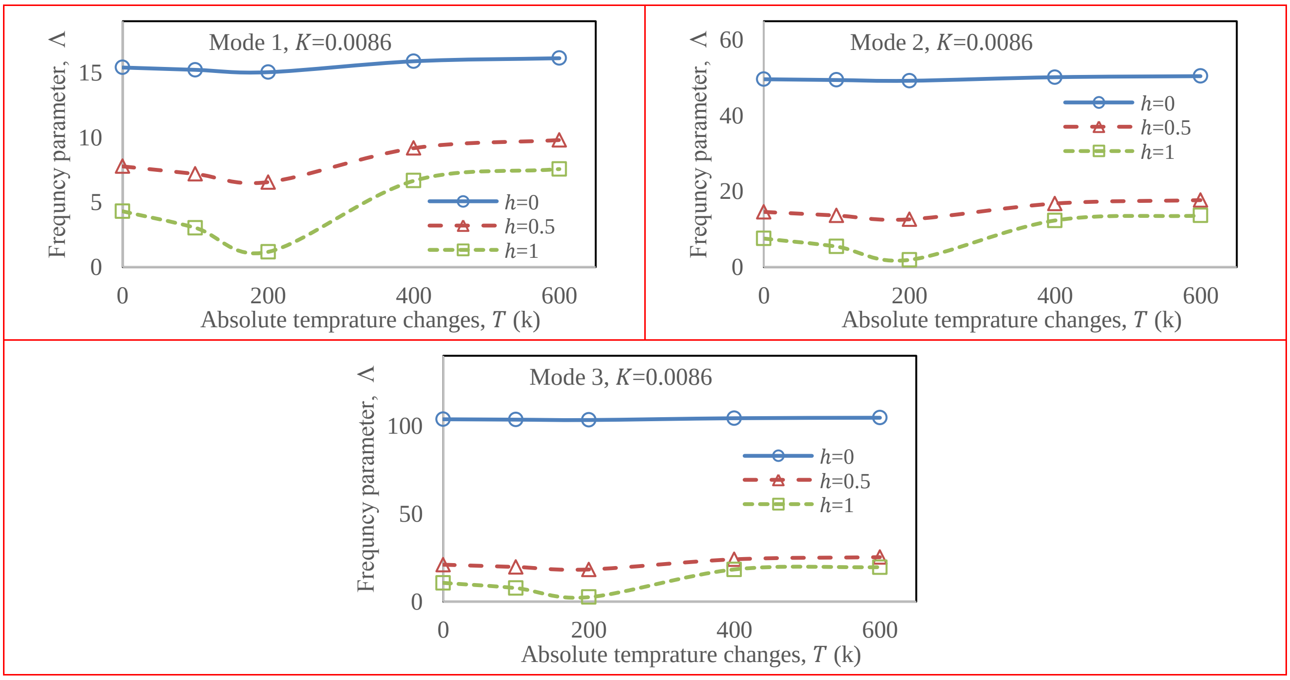

Figure 10. First three frequency parameters for a single-cracked CS beam versus temperature changes for different nonlocal parameters. ($K = 0.0086$ and $\varsigma = 0.3$).

It is observed that the clamped-clamped nanomaterial beam is stronger than the simply supported and the clamped-simply supported beams and its frequencies are higher than the two other cases even when the crack severity and the nonlocal parameter reach to high values at any temperature except the very low temperatures (i.e., $T = 200$). In the very low temperatures, approximately frequencies of all of the different beam supports approach each other as shown in Fig. 11.

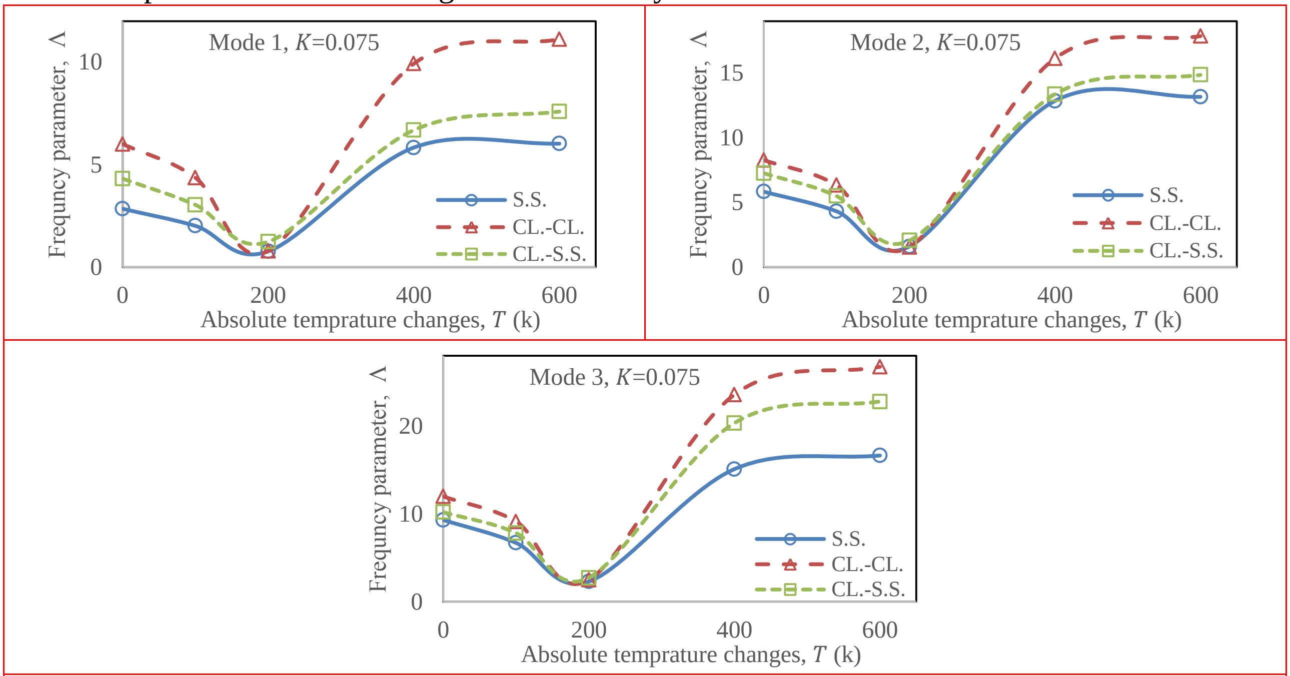

Figure 11. A comparison of first three frequency parameters of a single-cracked beam for different supports of SS, CC, and CS versus temperature changes. ($h = 1$, $K = 0.075$, and $\varsigma = 0.3$).

There is an investigation performed by (Ebrahimi and Mahmoodi, 2018) in which the effect of the thermal load on the multi-cracked beams is determined. Their investigation includes some significant mistakes that will change all of the results. They have not considered the thermal load in the compatibility equations which belong to the continuity of the shear and the continuity of the bending moment at the crack location. They have used the continuity equations of the bending moment and the shear force which belong to the cases in which the thermal load does not exist. The compatibility equations that have been used by them are as

- Continuity of the bending moment

$$\bar{W}_1''(\mathrm{b}) + \Lambda^2 h^2\, \bar{W}_1(\mathrm{b}) = \bar{W}_2''(\mathrm{b}) + \Lambda^2 h^2\, \bar{W}_2(\mathrm{b}) \quad (47)$$

- Continuity of the shear force

$$\bar{W}_1'''(\mathrm{b}) + \Lambda^2 h^2\, \bar{W}_1'(\mathrm{b}) = \bar{W}_2'''(\mathrm{b}) + \Lambda^2 h^2\, \bar{W}_2'(\mathrm{b}) \quad (48)$$

As it is seen in the Eqs. (47) and (48), there is not any parameter which belongs to the thermal load, that is the reason why their results were not sensitive to the temperature changes and they were not true. The true compatibility equations for the continuity of the bending moment and the continuity of the shear force are derived from the equation of motion and they are already obtained as Eqs. (39) and (40) in which q is the dimensionless thermal load as

- Continuity of the bending moment

$$(h^2\, q-1)\, \bar{W}_1''(\mathrm{b})-\Lambda^2 h^2\, \bar{W}_1(\mathrm{b})=(h^2\, q-1)\, \bar{W}_2''(\mathrm{b})-\Lambda^2 h^2\, \bar{W}_2(\mathrm{b})$$

- Continuity of the shear force

$$(h^2\, q-1)\, \bar{W}_1'''(\mathrm{b})-(\Lambda^2 h^2+\mathrm{q})\, \bar{W}_1'(\mathrm{b})=(h^2\, q-1)\, \bar{W}_2'''(\mathrm{b})-(\Lambda^2 h^2+\mathrm{q})\, \bar{W}_2'(\mathrm{b})$$

2 4. CONCLUSIONS

Following conclusions have been made from the results obtained throughout the present study:

- For the temperature change values higher than the room temperature, the frequencies are increased. Vice versa, for the temperature change values lower than the room temperature, the frequencies are decreased.
- Increasing the crack severity does not always result in decreasing the frequencies, because of the temperature changes. As the crack severity is increased the frequencies decrease because the flexibility of the beam is increased. But when the nonlocal parameter h is reached to a very high value (i.e. $h = 1$), the frequencies increase with increasing the crack severity at the temperatures lower and higher than the room temperature but not at the room temperature.

  It is concluded that a higher value of the nonlocal parameter does not always cause in decreasing the frequencies and the location of the crack is not always a tool to predict whether a certain frequency will be decreased or it will be increased because the temperature change has great effects on the frequencies.

  The outcomes of the investigation demonstrate that the clamped-clamped beam is stronger than the simply supported and the clamped simply supported beams and its frequencies are higher than the two other cases even when the crack severity and the nonlocal parameter reach the high values at any temperature except the very low temperatures (i.e. $T = 200$) in which approximately frequencies of all of the different beam supports approach each other.

Acknowledgments

The authors are grateful to the University of Salahaddin-Erbil for supporting this work.

Conflict of interests

The author declares that they have no competing interests.

Funding

The author declares that this paper does not have any funder.

References

ABDULLAH, S. S., HOSSEINI-HASHEMI, S., HUSSEIN, N. A. & NAZEMNEZHAD, R. 2020a. Effect of temperature on vibration of cracked single-walled carbon nanotubes embedded in an elastic medium under different boundary conditions. *Mechanics Based Design of Structures and Machines*, 1-26.

ABDULLAH, S. S., HOSSEINI-HASHEMI, S., HUSSEIN, N. A. & NAZEMNEZHAD, R. 2020b. Thermal stress and magnetic effects on nonlinear vibration of nanobeams embedded in nonlinear elastic medium. *Journal of Thermal Stresses*, 1-17.

AKBAS, S. D. 2018. Forced vibration analysis of cracked functionally graded microbeams. *ADVANCES IN NANO RESEARCH,* 6**,** 39-55.

AKBAŞ, Ş. D. 2017. Forced vibration analysis of functionally graded nanobeams. *International Journal of Applied Mechanics,* 9**,** 1750100.

EBRAHIMI, F. & BARATI, M. R. 2018. Vibration analysis of smart piezoelectrically actuated nanobeams subjected to magneto-electrical field in thermal environment. *Journal of Vibration and Control,* 24**,** 549-564.

EBRAHIMI, F. & MAHMOODI, F. 2018. Vibration analysis of carbon nanotubes with multiple cracks in thermal environment. *Advances in nano research,* 6**,** 57-80.

EBRAHIMI, F. & SALARI, E. 2015. Nonlocal thermo-mechanical vibration analysis of functionally graded nanobeams in thermal environment. *Acta Astronautica,* 113**,** 29-50.

ELTAHER, M., MAHMOUD, F., ASSIE, A. & MELETIS, E. 2013. Coupling effects of nonlocal and surface energy on vibration analysis of nanobeams. *Applied Mathematics and Computation,* 224**,** 760-774.

ERINGEN, A. C. 1972. Nonlocal polar elastic continua. *International journal of engineering science,* 10**,** 1-16.

ERINGEN, A. C. 1983. On differential equations of nonlocal elasticity and solutions of screw dislocation and surface waves. *Journal of applied physics,* 54**,** 4703-4710.

ERINGEN, A. C. & EDELEN, D. 1972. On nonlocal elasticity. *International Journal of Engineering Science,* 10**,** 233-248.

HAGHSHENAS, A. & ARANI, A. G. 2014. Nonlocal vibration of a piezoelectric polymeric nanoplate carrying nanoparticle via Mindlin plate theory. *Proceedings of the Institution of Mechanical Engineers, Part C: Journal of Mechanical Engineering Science,* 228**,** 907-920.

HOSSEINI-HASHEMI, S., KERMAJANI, M. & NAZEMNEZHAD, R. 2015. An analytical study on the buckling and free vibration of rectangular nanoplates using nonlocal third-order shear deformation plate theory. *European Journal of Mechanics-A/Solids,* 51**,** 29-43.

HUSSEIN, N. A., RASUL, H. A. & ABDULLAH, S. S. 2020. the Free vibration analysis of multi-cracked nanobeam using nonlocal elasticity theory. *Zanco Journal of Pure and Applied Sciences,* 32**,** 39-54.

KARLIČIĆ, D., CAJIĆ, M., MURMU, T. & ADHIKARI, S. 2015a. Nonlocal longitudinal vibration of viscoelastic coupled double-nanorod systems. *European Journal of Mechanics-A/Solids,* 49**,** 183-196.

KARLIČIĆ, D., JOVANOVIĆ, D., KOZIĆ, P. & CAJIĆ, M. 2015b. Thermal and magnetic effects on the vibration of a cracked nanobeam embedded in an elastic medium. *Journal of Mechanics of Materials and Structures,* 10**,** 43-62.

LOGHMANI, M. & YAZDI, M. R. H. 2018. An analytical method for free vibration of multi cracked and stepped nonlocal nanobeams based on wave approach. *Results in Physics,* 11**,** 166-181.

LOYA, J., LÓPEZ-PUENTE, J., ZAERA, R. & FERNÁNDEZ-SÁEZ, J. 2009. Free transverse vibrations of cracked nanobeams using a nonlocal elasticity model. *Journal of Applied Physics,* 105**,** 044309.

LU, P., LEE, H., LU, C. & ZHANG, P. 2006. Dynamic properties of flexural beams using a nonlocal elasticity model. *Journal of applied physics,* 99**,** 073510.

MURMU, T. & PRADHAN, S. 2009. Thermo-mechanical vibration of a single-walled carbon nanotube embedded in an elastic medium based on nonlocal elasticity theory. *Computational Materials Science,* 46**,** 854-859.

MURMU, T. & PRADHAN, S. 2010. Thermal effects on the stability of embedded carbon nanotubes. *Computational Materials Science,* 47**,** 721-726.

NAZEMNEZHAD, R. & HOSSEINI-HASHEMI, S. 2017. Exact solution for large amplitude flexural vibration of nanobeams using nonlocal Euler-Bernoulli theory. *journal of theoretical and applied mechanics,* 55**,** 649-658.

PEDDIESON, J., BUCHANAN, G. R. & MCNITT, R. P. 2003. Application of nonlocal continuum models to nanotechnology. *International Journal of Engineering Science,* 41**,** 305-312.

PHADIKAR, J. & PRADHAN, S. 2010. Variational formulation and finite element analysis for nonlocal elastic nanobeams and nanoplates. *Computational materials science,* 49**,** 492-499.

REDDY, J. 2007. Nonlocal theories for bending, buckling and vibration of beams. *International Journal of Engineering Science,* 45**,** 288-307.

REDDY, J. & PANG, S. 2008. Nonlocal continuum theories of beams for the analysis of carbon nanotubes. *Journal of Applied Physics,* 103**,** 023511.

ROOSTAI, H. & HAGHPANAHI, M. 2014. Vibration of nanobeams of different boundary conditions with multiple cracks based on nonlocal elasticity theory. *Applied Mathematical Modelling,* 38**,** 1159-1169.

SOLTANPOUR, M., GHADIRI, M., YAZDI, A. & SAFI, M. 2017. Free transverse vibration analysis of size dependent Timoshenko FG cracked nanobeams resting on elastic medium. *Microsystem Technologies,* 23**,** 1813-1830.

WANG, Q. 2005. Wave propagation in carbon nanotubes via nonlocal continuum mechanics. *Journal of Applied physics,* 98**,** 124301.

WANG, Q. & VARADAN, V. 2006. Vibration of carbon nanotubes studied using nonlocal continuum mechanics. *Smart Materials and Structures,* 15**,** 659.

WANG, Q., ZHOU, G. & LIN, K. 2006. Scale effect on wave propagation of double-walled carbon nanotubes. *International Journal of Solids and Structures,* 43**,** 6071-6084.

YAO, X. & HAN, Q. 2006. Buckling analysis of multiwalled carbon nanotubes under torsional load coupling with temperature change. *journal of engineering Materials and Technology,* 128**,** 419-427.

ZHANG, Y., LIU, G. & XIE, X. 2005. Free transverse vibrations of double-walled carbon nanotubes using a theory of nonlocal elasticity. *Physical Review B,* 71**,** 195404.

ZHANG, Y., LIU, X. & ZHAO, J. 2008. Influence of temperature change on column buckling of multiwalled carbon nanotubes. *Physics Letters A,* 372**,** 1676-1681.